Exobiology Extant Life Surveyor (EELS)

Kalind Carpenter[1]; Andrew Thoesen[2]; Darwin Mick[3]; Justin Martia[4]; Morgan Cable[5]; Karl Mitchell[6]; Sarah Hovsepian[7]; Jay Jasper[8]; Nikola Georgiev[9]; Rohan Thakker[10]; Ara Kourchians[11]; Brian Wilcox[12]; Michael Yip[13]; and Hamid Marvi[14]

[1]Jet Propulsion Laboratory, California Institute of Technology, Pasadena, CA
[2]School for Engineering of Matter, Transport and Energy, Arizona State Univ., Tempe, AZ
[3]School for Engineering of Matter, Transport and Energy, Arizona State Univ., Tempe, AZ
[4]School for Engineering of Matter, Transport and Energy, Arizona State Univ., Tempe, AZ
[5]Jet Propulsion Laboratory, California Institute of Technology, Pasadena, CA
[6]Jet Propulsion Laboratory, California Institute of Technology, Pasadena, CA
[7]Jet Propulsion Laboratory, California Institute of Technology, Pasadena, CA
[8]Jet Propulsion Laboratory, California Institute of Technology, Pasadena, CA
[9]Jet Propulsion Laboratory, California Institute of Technology, Pasadena, CA
[10]Jet Propulsion Laboratory, California Institute of Technology, Pasadena, CA
[11]Jet Propulsion Laboratory, California Institute of Technology, Pasadena, CA
[12]Jet Propulsion Laboratory, California Institute of Technology, Pasadena, CA
[13]Advanced Robotics and Controls Laboratory, School for Engineering, Univ. of California San Diego, La Jolla, CA
[14]School for Engineering of Matter, Transport and Energy, Arizona State Univ., Tempe, AZ

ABSTRACT

Cassini confirmed Enceladus's habitability for life as we know it. Enceladus plumes provide a unique pathway to sample from and potentially travel to an alien ocean. Enceladus offers many mobility challenges. At 1/87th Earth gravity the unconsolidated plume ejecta likely fluidizes when disturbed. This creates a buoyancy and swimming problem. Sintering of the ice grains challenges this and must be accounted for. The various models of how the plumes are driven provide a wide range of environments that may need to be traversed. Finally, fluid mobility is necessary. The exobiology extant life surveyor (EELS) architecture is developed to address this. It is composed of serially-replicated segments with encapsulated locomotion and bending. The concept uses a screw propulsion configuration that acts as tracks, gripping mechanisms, and propelling units especially under water. The resulting design is an adaptable solution to ocean world inspired terrains, fluidized granular media, enclosed labyrinthian environments, and liquids. This paper will cover an adaptable mobility system concept, current development, modeling, and experimental testing.

INTRODUCTION

Recently the active plumes from Enceladus have seen increased interest from the scientific community. Indications extrapolated from the presence and size of silica grains sensed by Cassini may likely be explained by hydrothermal reactions >90 C (Hsu et al (2015)). The Cassini spacecraft measured molecular hydrogen, which suggests the formation of ocean methane (Waite et al (2017)). A possible organic-rich film located at the top of the water table offers a target for instruments looking to find signs of life or detect motility. This film could consist of concentrated, complex, macromolecular masses above 200u to be found on Enceladus (Postberg et al (2018)). These conditions are similar to areas found on Earth rich in life. For example, at least one species of Earth methanogen still produced CH_4 in an analog Enceladus environment and withstood up to 50 bar of pressure (Taubner et al (2018)). Combined, this evidence makes Enceladus a potential sanctuary for extraterrestrial microbial life. If discovered, this breakthrough has numerous implications for both terrestrial and astrobiological sciences.

To attempt to access the ocean of Enceladus given the various models and ranges of parameters. We propose an adaptable snake like architecture that can change its effective diameter to meet the encounter terrain. The design is based on an active skin screw propelled robotic form with in-line center of mass. This concept is named the Exobiology Extant Life Surveyor (EELS) (Figure 1). The challenges of low gravity icy body mobility where unconsolidated media will fluidize when disturbed this architecture presents a novel approach to such a unique challenge. After introducing successful screw propelled vehicles we discuss the target environment and primary mission. Next, we discuss other applications of the robotic architecture. Various aspects of the architecture are then detailed, including mobility. Preliminary simulations of the architecture in Enceladus environment are performed. Finally, conclusions and next steps are discussed.

Figure 1: EELS robot

Screw propelled vehicles (SPV) have been proposed as a form factor for use in amphibious and icy environments. This style of propulsion system has been used before due to its unique ability to traverse difficult terrain containing materials such as snow, ice, mud or sand.

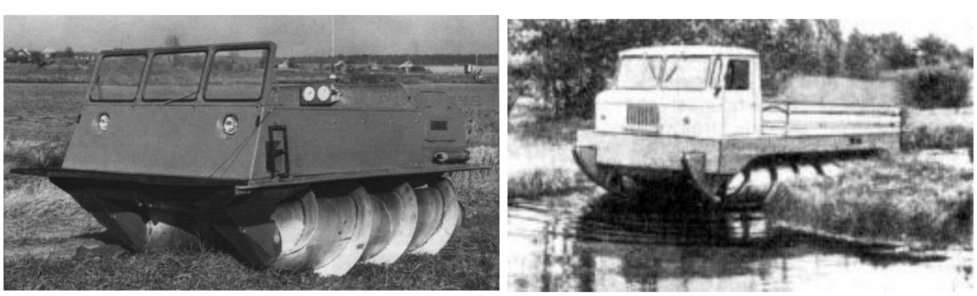

Figure 2: Left image: ZIL-2906, right image: GPI-72 (Image from Unusuallocomotion.com)

The ZIL-2906 shown in Figure 2 on the left, is an example of a Russian screw propelled vehicle used to retrieve Soyuz space capsules which often landed in areas that were difficult to reach with conventional vehicles. (Adlen (2018)). The GPI-72 shown in figure 2 on the right is another example of a screw-propelled vehicle used in arctic or colder regions.

Figure 3: Universal arctic rescue vehicle (URV) (Image M.Y. Sandakov Et. Al)

More recently, an improved screw-propelled vehicle design, shown in figure 3, has been developed for use in the arctic for rescue purposes; the universal arctic rescue vehicle (URV) uses an equalizing beam suspension which greatly improves the capabilities of screw-driven vehicles compared to the earlier designs (Koshurina et al (2016)). Other research has been done on the interactions of a rotary-screw vehicle and an icy surface. Helical blade shape of the geometry was the greatest contributing factor to the cutting force on the ice (Abramova et al (2018)).

Target Environment of EELS Architecture

Enceladus is the primary target environment of EELS to satisfy its overarching science goals: search for evidence of life. Enceladus plume vents are an optimal source for access to water which contain traces of organics (Postberg et al (2018)). The robots concept of operations is hierarchical to ensure the most pristine sample may be taken of the highest concentrations of material originating from the ocean. EELS may get a sample containing signs of life from the landing site; either way it will continue as far as it is able. To obtain a sample that will conclusively detect potential microbial life, EELS must be able to sample the surface of Enceladus, navigate Enceladus's icy terrain towards a vent opening while sampling the materials that falls out of the plume in concentric rings based off of mass, and attempt to sample directly from the plume. If none of these yield conclusive results or as an extended mission, EELS will attempt to navigate down through the vent conduits through the ice shell of Enceladus to explore the ice-water interface.

The thickness of the moon's ice shell is disputed, with early estimates of up to ~60 km (Iess et al., 2014; McKinnon, 2015), but a growing consensus that they might be closer to 20 km (Thomas et al., 2016; Čadek et al., 2016). The ice shell appears to be thinner at the thermally-active south pole, indicated by a topographic depression (Thomas et al., 2007), one of the early indications of a localized subsurface liquid reservoir (Collins and Goodman, 2007). Early estimates suggested only slight localized thinning from ~60 km to 30-40 km (Iess et al., 2014; McKinnon, 2015) but more recent studies imply <5 km thickness in the south polar region

(Čadek et al., 2016). The high tide point is estimated to be 10’s of meters to one kilometer from the surface.

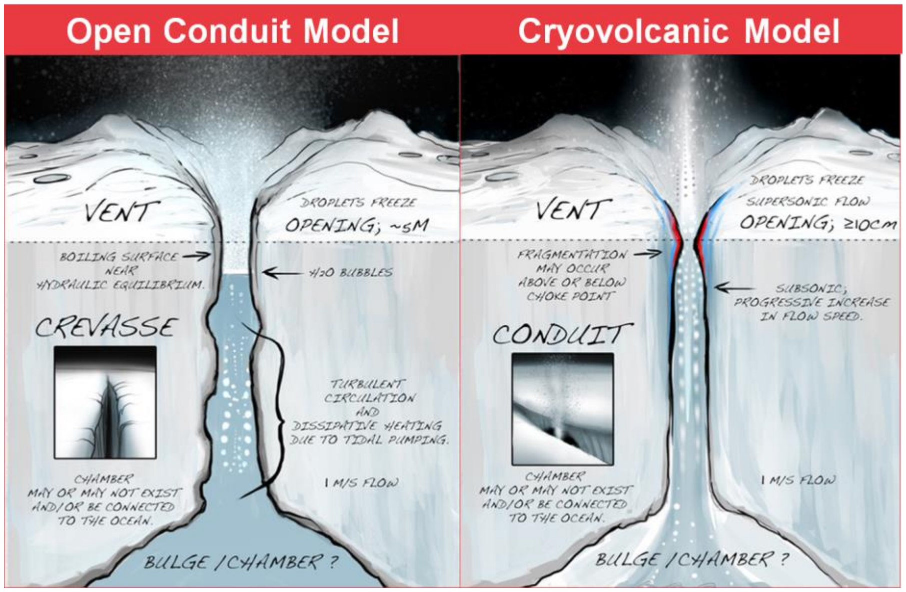

Figure 4: Schematic of Anticipated Scenarios

There are a range models that have been suggested for the ascent and eruption of water feeding the Enceladus plume. Kite and Rubin (2016) suggest large crevasses that open and close with tidal flexing, with hydraulically-supported liquid water pumped up and down turbulently, and the water-surface exposed directly to near-vacuum causing boiling which supplies a gas-dominated plume with liquid droplets (see fig. 4, left panel). Alternatively, Ingersoll and Nakajima (2016) evoke a controlled boiling model that results in much narrower fractures. However, neither of these take into account the role of dissolved volatiles, which appear to be present (e.g. Waite et al., 2017), and may cause activity to be more akin to terrestrial fire fountaining volcanism (we refer to this scenario as the *cryovolcanic* model, per Lopes et al., 2010). In this case, ascent is fueled by exsolution and expansion of volatiles from the liquid water during decompressional ascent (see fig. 4, right panel) within a relatively narrow conduit, passing through a nozzle and liquid water flashing to solid and vapor when pressure drops below the triple point (Mitchell et al., 2017 and in prep.). All of these cases likely have some evolution of the conduit through redeposition, abrasion and sublimation on/of the surrounding ice, which may lead to circularization of the vents and conduit structure from an initial fissure/fracture. It is anticipated that the vent connects to the subsurface ocean in all cases, but the extent to which the plume samples the ocean materials differs greatly.

The differences between these models impact the requirements on any robotic explorer. In the model of Kite and Rubin (2016), the opening may be a few meters wide, with water being pumped up and down within the vent and a boiling water surface at a depth controlled by hydraulic equilibrium. Dynamic pressures would be very weak (Mitchell et al., 2017). In other models, the throat may be considerably smaller, of order ~10 cm, as a fissure (Ingeroll and Nakajima, 2016) or as circular vents (Mitchell et al., 2017, in prep.); Supersonic flow within the conduit is possible, and dynamic pressures may be considerable, potentially a daunting 10^7

Pascals (Mitchell et al., 2017). This relationship informs an architecture that may fall or repel down a wide crevasse, reacting to increasingly large forces down to the centimeter range. Local gravity is one eighty seventh that of Earth, and easily overcome by most of the range of potential plume forces. The greatest possible plume forces bring more scientifically relevant samples to the surface so a mission may achieve its sampling goals regardless. As the dynamic pressure goes up, so does the static pressure, this means that the ice is heated and pressurized by the flow to be above the triple point. These cases make it possible to test solutions on Earth as a relevant environment.

Secondary Applications for EELS Architecture

Along with Enceladus applications, EELS can be implemented on Earth. A major source of melt comes from rivers and streams that run through glaciers. EELS is designed specifically for icy and wet terrain. With the right sensors equipped, EELS could swim through these rivers, tunnel through glacier cracks, and even follow runoff from its origin to its final destination (Figure 3).

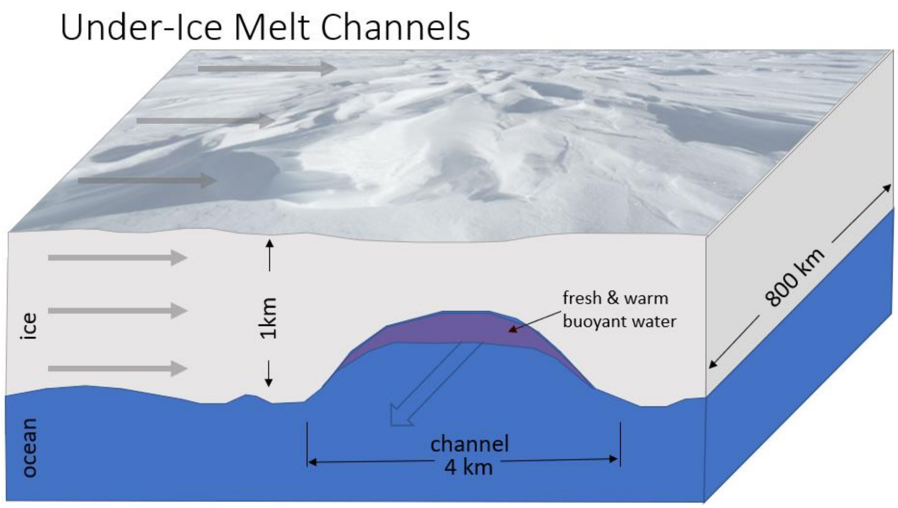

Figure 5: Earth Melt Channels (Image courtesy of Dr. Alex Gardner)

Overall, EELS can make significant contributions to collecting data that relates glacier shrink to runoff rates. Bathymetry below ice shelves helps show where warm water flows and is highly necessary for accurately simulating ice sheet advance because glacier flow is dependent on the geometry of the ice sheet itself. Unfortunately, bathymetry is difficult to measure due to roughly 500 m of ice capping and the daunting spatial scale of ice sheets. EELS could be deployed through holes in the ice created by inexpensive "hot water" drills thus enabling more accurate and complete bathymetry measurements under previously completely unknown ice sheets.

EELS can also be implemented for avalanche disaster relief. Between the years 1994 and 2003, the median annual mortality rate for snow avalanches was 141. Wearable tools and devices have been created to bring this number down. The two most prominent are an avalanche transceiver, to make it easier to find victims, and an avalanche airbag, which keeps victims from being crushed. Both of these methods have proved to be effective. The avalanche airbag decreased mortality rates by 16% and the avalanche transceiver by 15.4%. However, mortality is still at 55.2% (Brugger et al (2007)). EELS could be used to help locate and even assist buried victims. This would be much safer than sending humans into the field while the snow is still loose and liable to avalanche a second time.

Multi-Modal Mobility

The mobility of EELS will be holonomic to allow for high accuracy in steering. The first mobility modality is traversing the surface of Enceladus. In high slip fluidized granules, EELS will take advantage of its screws to to push the grains back propelling EELS forward. The second modality is descending the icy crevasse. In an open fracture system, EELS extends across the gap near the initiation point of a fracture, out of the stream line, and pushes two end screw mechanisms on each side into the walls. This anchors the craft to the crevasse walls by means of outward pushing forces. The robot then drives into the plume streamline, descending against the flow. In the vent, the threads bite into the side walls, providing the necessary anchoring force against the plume jet forces. The system is designed to provide enough force to induce pressure melting even though the cutting and heating from conductive coupling will provide a greater contribution to ice penetration.

The robot descends by rotating the threads, creating a spiraling motion continuing downward. The snake-like body adapts by elongating its spiral pitch and changing the angle between joints to describe a wide circle down to one of a single body diameter. Using force and position control EELS acts as a circular spring, pushing outwards, and descending slowly as one might imagine down a chimney (see Figure 4). Once at the bottom, EELS may find itself impeded by the throat at the bottom of the crevasse. In this case, EELS can act as a self-driven screw where the angle actuators no longer have mechanical disadvantage and can push the threads most forcefully into the ice reacting the greatest potential force and letting the mechanical advantage of the threads to pull the robot through the choke point. The choke point is likely near the high tide mark of Enceladus which occurs every 16 hours. Once into the water EELS may swim to access the ocean underneath.

Figure 6: EELS computer animation of descent through crevasse to subsurface ocean

Controls and Sensing

The rotation of the screws is balanced by counter-rotating secondary units that provide anchoring and thrust. In particular, each segment of EELS has two screws, each rotating opposite directions. Counter-rotation allows EELS to maintain a controlled forward path. In addition, this design will balance any created moments, allowing for a single forward thrust. In the case of wide caverns or slip of the leading screw unit, the additional Archimedes screw units provide grip until the leading units find their next secure position. If one segment fails to secure itself, the others can compensate for the temporary loss. Force and position control of the joints allows adaptability without perfect knowledge of the geometry of the environment; the robot can naturally conform its shape to the size of the vent (Figure 7). This is used to move the drive screws in any direction to maintain a desired outward force on crevasse walls, which makes the screw threads grip the surface and directs the robot around bends, enabling branch following of a conduit across wide gaps. Furthermore, a proprioceptive feedback loop may also be used. This architecture has never been realized in any other robotic applications to this point.

As a part of its highly adaptable design, and fast rate of vent descent, EELS must navigate autonomously. In order to do this, it will follow the source of highest mass flux working under the assumption that the source of the flow is the subsurface ocean. By adapting its gait to maintain control and pressure exerted against the walls of the vent, EELS is designed to use automated science target identification to determine high science return targets for sampling. It will autonomously acquire samples and prepare them for analysis. Furthermore, EELS will be able to summarize data application and send prioritized information to Earth first as well as do its own science activity planning.

Figure 7: Left image: EELS Prototype for Force Compliance Testing demonstrating vertical traversal in a barrel. Right image: load leveling validation.

To date the initial prototype has gone through ground and barrel testing. A full version is currently being assembled for testing on ice in a walk-in freezer. The design and results of this will be presented in a future publication.

Characterization of Icy Environments for Simulation

Discrete element method (DEM) coupled to multi-body dynamics (MBD) simulations introduce a unique capability to evaluate dynamic robots interacting with complex granular environments. These simulations can provide insights on body drag, optimization of screw shape, and other kinematic and dynamic aspects in the target gravity. Particles are treated as agglomerates of spheres; MBD-DEM simulations can select frictional and material properties of the environment among others to create a computational comparison. Characterizing the icy terrain of Enceladus is a critical step for determining analogue testing environments as well as creating accurate simulations.

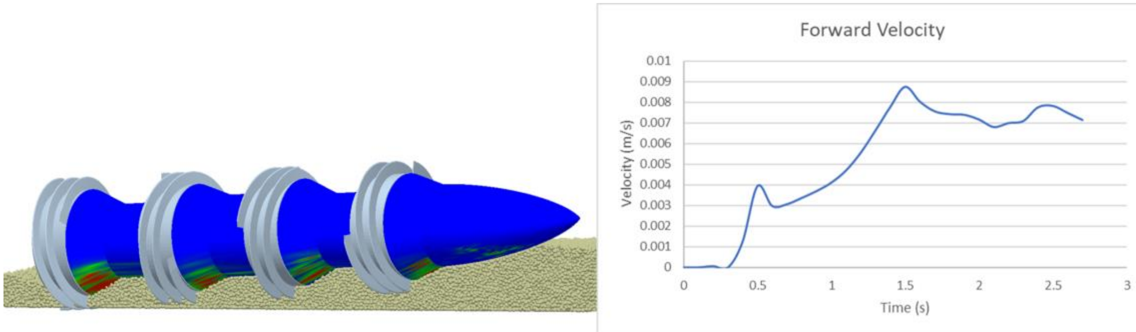

Figure 8: EELS simplified architecture is displayed in DEM environment with simulated velocity response to Enceladus gravity and ice grains

Ice properties, as both a solid material and granular media, can be hard to determine as they fluctuate based on temperature. It has been found that a Young's Modulus of 9 GPa, a 0.33 Poisson's ratio, and an ice density of 930 kg/m^3g can be used as an acceptable starting point for ice characteristics (Randhawa (2018). Other parameters vary; simulations from the literature have used 0.01 - 0.88 as a coefficient of restitution (Morgan et al (2015)). In Earth applications, the static friction for ice-ice interaction has been defined as 0.35 (Paavilainen (2006)). However, this coefficient has been estimated to be as high as 0.73 on Enceladus due to cryogenic temperatures (Schulson and Fortt (2012)). Schulson et al. found that at faster speeds (1 mm/s), the coefficient of friction measured was 0.76 for 1 mm diameter grains and was reduced to 0.7 for 8 mm diameter grains. Conclusions from the same body of research have characterized shear/normal stress relationships in granular ice as highly velocity dependent and in-house testing from our work agrees with this as well.

Using the available parameters and 3 mm agglomerate models (two- and three-sphere shape composites), preliminary MBD-DEM simulations were performed on a simplified craft using the counter-rotating dual screw design in an Enceladus gravity environment (Figure 7). These preliminary simulations serve two purposes. The first is to provide a first-order estimate of how the architecture may perform in a target environment. The second is to evaluate the design for improvement. Locating the majority of the robotic mass in-line with the propulsive vector inherently creates more stability, allowing for speeds above 8 mm/s (Figure 7). Due to the accumulation of particles in front of screw bases, a dip in the velocity occurs and it settles around 7.5 mm/s. The next iteration will see a variation on screw pitch, as well as body shape for better drag resistance.

Conclusion and Future Work

In conclusion, Enceladus's hydrothermal activity and resultant organic molecules make it a likely home for microbial life. This, plus its relatively known environment makes Enceladus an optimal candidate for a mission. The unique design of EELS offers advanced capabilities in icy environments and enables the exploration of this icy moon. Furthermore, its maneuverability in cavernous environments makes EELS an applicable candidate for Earth focused missions such as measuring glacier melt and avalanche disaster relief. Several avenues of future work can be pursued in parallel. In particular, the dynamic response of the robotic system to an Enceladus analogue will be tested with a granular media holding similar properties. Moreover, screw shape will be evaluated in simulation and experiment to strike an ideal design balance between solid ice wheel traversal, granular screw traversal, and outward pressure descending down crevasses. This includes evaluation of candidate materials such as bulk metallic glasses. Finally, additional MBD-DEM simulations will be run in parallel with experiments to observe the responses in an Enceladus gravity which may lead to insights otherwise ignored.

REFERENCES

Abramova, E., Mashorin, G., Molev, Y., and Sogin, A. (2018). The simulations of helical blade interaction with ice. In MATEC Web of Conferences (Vol. 245, p. 17002). EDP Sciences.

Adlen, N. 2018, The Dangerous Past: The ZIL-2906 – the Screw Drive, All-Terrain Russian Soviet Awesomeness, tfloffroad.com, accessed 8 August 2020, <https://www.tfloffroad.com/2018/08/the-dangerous-past-the-zil-2906-the-screw-drive-all-terrain-russian-soviet-awesomeness/>.

Barraquand, J., Langlois, B., and Latombe, J. C. (1992). Numerical potential field techniques for robot path planning. *IEEE transactions on systems, man, and cybernetics*, *22*(2), 224-241.

Bliss, A., Hock, R., and Radić, V. (2014). Global response of glacier runoff to twenty-first century climate change. *Journal of Geophysical Research: Earth Surface*, *119*(4), 717-730.

Bolton, S. J. (2017). Cassini finds molecular hydrogen in the Enceladus plume: evidence for hydrothermal processes. *Science*, *356*(6334), 155-159.

Brugger, H., Etter, H. J., Zweifel, B., Mair, P., Hohlrieder, M., Ellerton, J., Elsensohn, F., Boyd, J. Sumann, G., and Falk, M. (2007). The impact of avalanche rescue devices on survival. *Resuscitation*, 75(3), 476-483.

Burget, F., Hornung, A., and Bennewitz, M. (2013, May). Whole-body motion planning for manipulation of articulated objects. In 2013 IEEE International Conference on Robotics and Automation (pp. 1656-1662). IEEE.

Čadek, O., et al. (2016) Enceladus' nternal ocean and ice shell constrained from Cassini gravity, shape and libration data. *Geophys. Res. Lett.* 43(11), 5653-5660.

Collins, G. C., and Goodman, J. C. (2007) Enceladus' south polar sea. *Icarus* 189, 72–82.

Crespi, A., and Ijspeert, A. J. (2008). Online optimization of swimming and crawling in an amphibious snake robot. *IEEE Transactions on Robotics*, *24*(1), 75-87.

Cully, A., Clune, J., Tarapore, D., and Mouret, J. B. (2015). Robots that can adapt like animals. *Nature*, *521*(7553), 503.

Diedam, H., Dimitrov, D., Wieber, P. B., Mombaur, K., and Diehl, M. (2008, September). Online walking gait generation with adaptive foot positioning through linear model predictive control. In 2008 IEEE/RSJ International Conference on Intelligent Robots and Systems (pp. 1121-1126). IEEE.

GPI-72 https://www.unusuallocomotion.com/pages/locomotion/screw-propelled-vehicles.html.

Grizzle, J. W., Chevallereau, C., Sinnet, R. W., and Ames, A. D. (2014). Models, feedback control, and open problems of 3D bipedal robotic walking. *Automatica*, *50*(8), 1955-1988.

Gong, C., Travers, M. J., Astley, H. C., Li, L., Mendelson, J. R., Goldman, D. I., and Choset, H. (2016). Kinematic gait synthesis for snake robots. *The International Journal of Robotics Research*, *35*(1-3), 100-113.

Higa, M., Arakawa, M., and Maeno, N. (1996). Measurements of restitution coefficients of ice at low temperatures. *Planetary and space science*, *44*(9), 917-925.

Hsu, H. W., Postberg, F., Sekine, Y., Shibuya, T., Kempf, S., Horányi, M., Juhász, A., Altobelli, N., Suzuki, K., Masaki, Y., Kuwatani, T., Tachibana, S., Sirono, S., Moragas-Klostermeyer, G., and Srama, R. (2015). Ongoing hydrothermal activities within Enceladus. *Nature*, *519*(7542), 207.

Iess, L., et al. (2014) The gravity field and interior structure of Enceladus. *Science* 344, 78–80.

Kennedy, F. E., Schulson, E. M., and Jones, D. E. (2000). The friction of ice on ice at low sliding velocities. *Philosophical Magazine A*, *80*(5), 1093-1110.

Kite, E. S., and Rubin, A. M. (2016) Sustained eruptions on Enceladus explained by turbulent dissiptation in tiger stripes. *Proc. Nat. Acad. Sci*, 113(15), 3972-3975.

Koshurina, A. A., Krasheninnikov, M. S., and Dorofeev, R. A. (2016). Strength calculation and analysis of equalizer beam embodiments for the operated equalizing beam suspension of the Universal rotor-screw rescue vehicle for the arctic. *Procedia Engineering*, *150*, 1263-1269.

Liang, H., Martin, J. M., and Mogne, T. L. (2003). Experimental investigation of friction on low-temperature ice. *Acta materialia*, *51*(9), 2639-2646.

Lopes, R. M. C., Mitchell, K. L., Williams, D., and Mitri, G. (2010) Beyond Earth: How extra-terrestrial volcanism has changed our definition of a volcano. In *Special Paper of the Geological Society of America,* 470, 11-30.).

Melo, K., Paez, L., Hernandez, M., Velasco, A., Calderon, F., and Parra, C. (2011, October). Preliminary studies on modular snake robots applied on de-mining tasks. In IX Latin American Robotics Symposium and IEEE Colombian Conference on Automatic Control, 2011 IEEE (pp. 1-6). IEEE.

Sandakov, M.Y., Mukhina, M.L., Koshurina, A.A., Krasheninnikov, M.S., and Dorofeev, R.A. (2015) The study of seaworthiness of universal rescue vehicle with rotary screw propeller. International Conference on Advanced Manufacturing Industry Application.

McKinnon, W. B. (2015) Effect of Enceladus's rapid synchronous spin on interpretation of Cassini gravity. *Geophys. Res. Lett.* 42, 2137–2143.

Mitchell, K. L., Ono, M., Parcheta, C., and Iacoponi, S. (2017) Dynamic pressure at Enceladus vents and implications for vent and conduit in-situ studies. *Lunar planet. Sci. XLVIII*, Lunar and Planetary Institute, Houston, TX, Abstract #2801.

Morgan, D., Sarracino, R., McKenna, R., and Thijssen, J. W. (2015). Simulations of ice rubbing against conical structures using 3D DEM. In Proceedings of the International Conference on Port and Ocean Engineering Under Arctic Conditions.

Ostrowski, J., and Burdick, J. (1998). The geometric mechanics of undulatory robotic locomotion. *The international journal of robotics research*, *17*(7), 683-701.

Paavilainen, J., Tuhkuri, J., and Polojärvi, A. (2006). Discrete element simulation of ice pile-up against an inclined structure. In IAHR 18th International Symposium on Ice (pp. 177-184).

Polojärvi, A., Tuhkuri, J., and Pustogvar, A. (2015). DEM simulations of direct shear box experiments of ice rubble: force chains and peak loads. *Cold Regions Science and Technology*, *116*, 12-23.

Postberg, F., Khawaja, N., Abel, B., Choblet, G., Glein, C. R., Gudipati, M. S., Henderson, B. L., Hsu, H., Kempf, S., Fabian, K., Moragas-Klostermeyer, G., Magee, B., Nöll, L., Perry, M., Reviol, R., Schmidt, J., Srama, R., Stolz, F., Tobie, G., Trieloff, M., and Waite, J. H. (2018). Macromolecular organic compounds from the depths of Enceladus. *Nature*, *558*(7711), 564.

Randhawa, K. S. (2018). *The measurement of the Young's modulus of ice with ultrasonic waves* (Doctoral dissertation, Technische Universität Hamburg).

Schmidt, J., Brilliantov, N., Spahn, F., and Kempf, S. (2008) Slow dust in Enceladus' plume from condensation and wall collisions in tiger stripe fractures. *Nature* 451(7179), 685–688.
Schulson, E. M., and Fortt, A. L. (2012). Friction of ice on ice. *Journal of Geophysical Research: Solid Earth*, *117*(B12).
Taubner, R. S., Pappenreiter, P., Zwicker, J., Smrzka, D., Pruckner, C., Kolar, P., Bernacchi, S., Seifart, A. H., Krajete, A., Bach, W., Peckmann, J., Paulik, C., Firneis, M. G., Schleper, C., and Rittmann, S. (2018). Biological methane production under putative Enceladus-like conditions. *Nature communications*, *9*(1), 748.
Thomas, P. C., et al. (2007) Shapes of the saturnian icy satellites and their significance. *Icarus* 190, 573–584.
Thomas, P. C., Tajeddine, R., Tiscareno, M. S., Burns, J. A., Joseph, J., Loredo, T. J., Helfenstein, P., and Porco, C. (2016) Enceladus's measured physical libration requires a global subsurface ocean. *Icarus* 264, 37–47.
Travers, M., Whitman, J., and Choset, H. (2018). Shape-based coordination in locomotion control. *The International Journal of Robotics Research*, *37*(10), 1253-1268.
Waite, J. H., et al. (2017) Cassini finds molecular hydrogen in the Enceladus plume: Evidence for hydrothermal processes. *Science*, 356(6334), 155-159.
Waite, J. H., Glein, C. R., Perryman, R. S., Teolis, B. D., Magee, B. A., Miller, G., Grimes, J., Perry, M. E., Miller, K. E., Bouquet, A., Lunine, J. I., Brockwell, T., Wallen-Russell, C., and Lishman, B. (2016). The friction of saline ice on aluminium. *Advances in tribology*, 2016.